



# Heat and momentum transfer for compact louvered fin-and-tube heat exchangers in wet conditions

Chi-Chuan Wang<sup>a,\*</sup>, Yur-Tsai Lin<sup>b</sup>, Chi-Juan Lee<sup>b</sup>

<sup>a</sup>*Energy and Resources Laboratories, Industrial Technology Research Institute, Hsinchu, Taiwan*

<sup>b</sup>*Department of Mechanical Engineering, Yuan-Ze University, Tawuyuan, Taiwan*

Received 31 May 1999

## Abstract

The air side performances of two louvered fin surfaces under dehumidifying conditions were examined in this study. The test results indicated that the effect of fin pitch on the heat transfer performance is comparatively small, and the friction factors increase significantly with fin pitch for fully wet conditions. The effect of inlet relative humidity on the sensible heat transfer performance is negligible. However, there is a detectable effect of inlet condition on the friction factors for type (I) louver due to condensate retention. A correlation of heat, momentum, and mass transfer was proposed to correlate the present database with a mean deviation of 5.94%, 6.1%, and 7.89%, respectively. © 2000 Elsevier Science Ltd. All rights reserved.

## 1. Introduction

In typical air-conditioning heat exchangers like fan-coil unit or evaporator, where surface temperature may be operated below its corresponding dew point, simultaneous heat and mass transfer occurs on the surface, and water condensate is formed. The air-flow across the heat exchanger may interact with the water condensate which makes the flow pattern very complicated. As a result, significant change of the heat transfer and friction characteristics is likely to occur under dehumidifying conditions. Many researches and analyses had been devoted to this problem yet the fundamental basis for the methods now in use is still debatable. As pointed out by Wang et al. [1], the data reduction for experimental work in the open literature

used different approaches and hence, significant errors may be encountered when one tries to use other's data with different reduction method. Moreover, some methods are physically inappropriate, it is hard and irrelevant to compare the test results from one to another.

Recently, use of compact fin-and-tube heat exchangers which incorporated with enhanced fin patterns like louver and offset strip is quite common in the commercial/residential application since these fin patterns are cost-effective. The louver fin, as shown in Fig. 1, is especially popular owing to its superior performance and low cost. There are several investigations associated with the air side performance of the louver fin, most of which were related to fully dry conditions [2–6]. Experimental data reported in literature were very limited for louver fin under dehumidifying [7–9]. Notice that the fully wet conditions exist when the fin surface temperatures are below its corresponding inlet dew point temperatures. The main objective of the present study is to present air side performance of

\* Corresponding author. Tel.: +886-3-591-6294; fax: +886-3-582-0250.

E-mail address: ccwang@itri.org.tw (C.-C. Wang).

### Nomenclature

$A_c$	minimum free flow area		heat transfer rate $\dot{Q}_a$ .
$A_o$	total surface area	$\dot{Q}_a$	air side heat transfer rate
$A_{p,o}$	outer surface area of tubes	$\dot{Q}_w$	water side heat transfer rate
$C_p$	heat capacity for air	$Sc$	Schmidt number
$D_c$	tube outside diameter, including collar ( $D_c = D_o + 2\delta_f$ )	$Sh$	Shwood number
$D_h$	hydraulic diameter	$Re_{D_i}$	Reynolds number based on inside diameter
$D_i$	tube inside diameter	$Re_{D_c}$	Reynolds number based on $D_c$
$D_o$	tube outside diameter	RH	relative humidity
$f$	friction factor	RT	refrigeration tons
$F_p$	fin pitch	$T$	temperature
$G_c$	maximum mass velocity based on minimum flow area	$T_{db}$	dry bulb temperature
$h_{c,o}$	sensible heat transfer coefficient for wet coils	$T_a$	air temperature
$h_d$	mass transfer coefficient	$T_w$	water temperature
$h_{o,w}$	total heat transfer coefficient for wet external fin	$U_{o,w}$	overall heat transfer coefficient (enthalpy-based)
$i_{g,t}$	enthalpy of saturated water vapor evaluated at mean air temperature	$W$	humidity ratio
$j$	the Colburn factor	$W_{s,w}$	humidity ratio of saturated moist air evaluated at condensate temperature
$L$	depth of the heat exchanger	$x_p$	tube wall thickness
$Le$	ratio of $h_{c,o}$ and $h_d C_p$	$\delta_f$	fin thickness
$L_h$	louver height	$\eta_{f,wet}$	wet fin efficiency
$L_p$	louver pitch	$\theta$	louver angle, $\tan \theta = L_h/L_p$
$\dot{m}_{air}$	mass flow rate of airflow	$\mu_f$	dynamic viscosity of water
$\dot{m}_w$	mass flow rate of water flow	$\rho_i$	mass density of inlet air
$N$	the number of tube row	$\rho_o$	mass density of outlet air
$p$	system pressure	$\rho_m$	mean mass density of air
$\Delta P$	pressure drop	$\sigma$	contraction ratio
$P_l$	longitudinal tube pitch	$\Gamma$	mass flow rate per unit width of the tube
$P_t$	transverse tube pitch		
$\dot{Q}_{avg}$	mathematical average heat transfer rate for water side heat transfer rate $\dot{Q}_w$ and air side		

### Subscripts

Exp	experimental value
Cor	correlation value

louver fin pattern extensively and to propose their correlations under fully wet conditions to use consistent approach to reduce the air side data with the enthalpy-based method as proposed by Threlkeld [10] and recommended recently by Kandlikar [11].

## 2. Test unit and experimental apparatus

Table 1 shows the detailed geometry of the present plate fin-and-tube heat exchangers. The test fin-and-tube heat exchangers are tension wrapped having a “L” type fin collar. The test samples consisted of 10 louver fin-and-tube heat exchangers. Detailed dimensions of the louver fin patterns are illustrated in Fig. 1. The height of louver,  $L_h = 1.07$  mm, is the same for both louver fin pattern. The major differences between

these two louvers are (1) the longitudinal tube pitch for type (I) is 19.05 mm while type (II) is 22 mm; (2) the major louver pitch for type (I) is 2.35 mm whereas for type (II) is 2.0 mm; and (3) the number of louvers for type (I) in one-row is less than that of type (II) by 2. The test conditions of the inlet air are as follows:

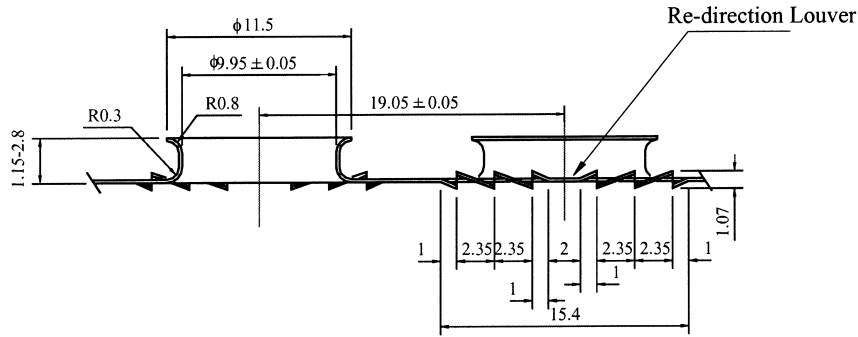
Dry-bulb temperatures of the air	$27 \pm 0.5^\circ\text{C}$
Inlet relative humidity for the incoming air	50% and 90%
Inlet air velocity	$0.4\text{--}3.5 \text{ m}\cdot\text{s}^{-1}$
Inlet water temperature	$6.5 \pm 2^\circ\text{C}$
Water velocity inside the tube	$1.5\text{--}2.0 \text{ m}\cdot\text{s}^{-1}$

The test conditions approximate those encountered with typical fan-coils and evaporators of air-condition-

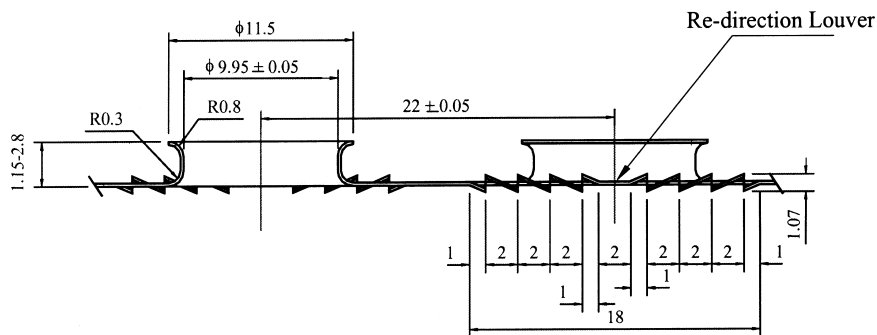
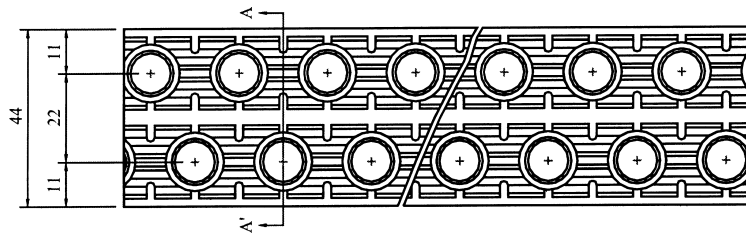
ing applications. Schematic diagram of the experimental air circuit assembly is shown in Fig. 2. It consists of a closed loop wind tunnel in which air is circulated by a variable speed centrifugal fan (7.46 kW, or 10 HP accordingly). The air duct is made of galvanized steel sheet and has a 850 mm × 550 mm cross-section. The dry-bulb and wet-bulb temperatures of the inlet air are controlled by an air-ventilator that can provide a cooling capacity up to 21.1 kW. The air flow rate measurement station is an outlet chamber setup with multiple

nozzles. This setup is based on the ASHRAE 41.2 standard [12]. A differential pressure transducer is used to measure the pressure difference across the nozzles. The air temperatures at the inlet and exit zones across the sample heat exchangers are measured by two psychrometric boxes constructed based on the ASHRAE 41.1 standard [13].

The working medium on the tube side is cold water. A thermostatically controlled reservoir provides the cold water at selected temperatures. The temperature



**Type (I),  $P_t = 25.4 \text{ mm}$ ,  $P_l = 19.05 \text{ mm}$**



**Type (II),  $P_t = 25.4 \text{ mm}$ ,  $P_l = 22 \text{ mm}$**

Fig. 1. Detailed dimensions of the test louver fin patterns.

Table 1  
Geometric dimensions of the louver fin-and-tube heat exchangers<sup>a</sup>

No.	Fin pattern	$F_p$ (mm)	$D_c$ (mm)	$P_1$ (mm)	$P_2$ (mm)	$L_h$ (mm)	$L_p$ (mm)	$L_p/F_p$	Row no.
1	Louver (I)	1.21	10.33	25.4	19.05	1.07	2.35	1.94	1
2	Louver (I)	1.82	10.33	25.4	19.05	1.07	2.35	1.29	1
3	Louver (I)	2.49	10.33	25.4	19.05	1.07	2.35	0.94	1
4	Louver (I)	1.21	10.33	25.4	19.05	1.07	2.35	1.94	2
5	Louver (I)	1.78	10.33	25.4	19.05	1.07	2.35	1.32	2
6	Louver (I)	2.42	10.33	25.4	19.05	1.07	2.35	0.97	2
7	Louver (II)	1.21	10.33	25.4	22	1.07	2	1.65	1
8	Louver (II)	2.47	10.33	25.4	22	1.07	2	0.81	1
9	Louver (II)	1.21	10.33	25.4	22	1.07	2	1.65	2
10	Louver (II)	2.49	10.33	25.4	22	1.07	2	0.8	2

<sup>a</sup> Nominal tube diameter before expansion is 9.52 mm. All the test surfaces were not hydrophilic coated. There are no hydrophilic coating of the fin surfaces. The maximum deviation due to manufacturing accuracy of the louver height is  $\pm 0.05$  mm. A manual counting process is performed in each test samples for their exact fin number, the fin pitch is obtained by dividing the width of the test samples to the exact fin numbers. Tube wall thickness: 0.31 mm. Fin thickness: 0.115 mm. Fin material: aluminum ( $k = 204 \text{ m}\cdot\text{W}\cdot\text{K}^{-1}$ ). Tube material: copper.

differences on the water side are measured by two pre-calibrated RTDs. The water volumetric flow rate is measured by a magnetic flow meter with a  $\pm 0.001$  L/s precision. All the temperature measuring probes are resistance temperature device (Pt100), with a calibrated accuracy of  $\pm 0.1^\circ\text{C}$ . In the experiments, only those data that satisfy the ASHRAE 33-78 requirements (namely, the energy balance conditions,  $|\dot{Q}_w - \dot{Q}_a|/\dot{Q}_{\text{avg}}$ , is less than 0.05, where  $\dot{Q}_w$  is the water-side heat transfer rate and  $\dot{Q}_{\text{avg}}$  is the mathematical average heat transfer rate for  $\dot{Q}_w$  and air-side heat transfer rate  $\dot{Q}_a$ ), are considered in the final analysis. Uncertainties reported in the present investigation, fol-

lowing the single-sample analysis proposed by Moffat [14], are tabulated in Table 2.

### 3. Analysis

Details of the reduction process can be found from the previous studies by Wang et al. [1] and Wang and Chang [9]. Notice that the Threlkeld method is an enthalpy-based reduction method. A brief description of the reduction of heat and mass transfer is given as follows.

The overall heat transfer coefficient is related to the individual heat transfer resistance [15] as follows:

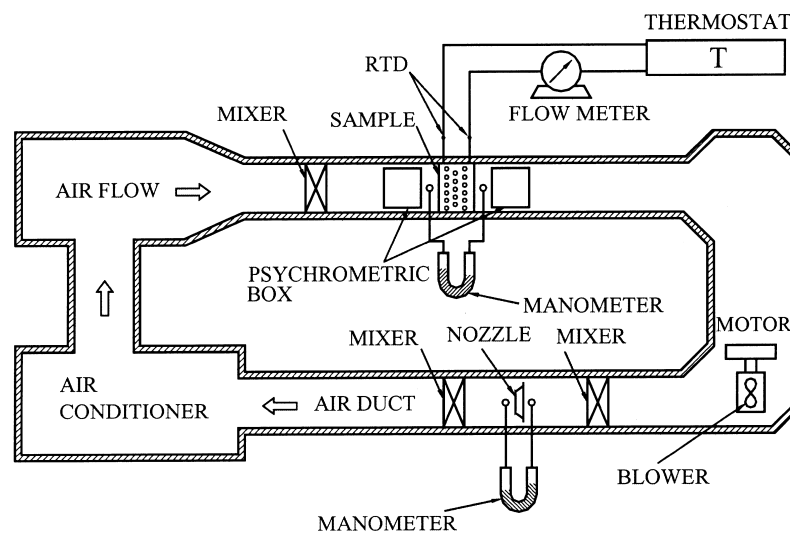


Fig. 2. Schematic of the test setup.

Table 2  
Summary of estimated uncertainties

Primary measurements		Derived quantities		
Parameter	Uncertainty	Parameter	Uncertainty $Re_{D_c} = 500$	Uncertainty $Re_{D_c} = 300$
$\dot{m}_{air}$	0.3–1%	$Re_{D_c}$	$\pm 1.0\%$	$\pm 0.62\%$
$\dot{m}_w$	0.5%	$Re_{D_i}$	$\pm 0.73\%$	$\pm 0.86\%$
$\Delta P$	0.5%	$f$	$\pm 13.7\%$	$\pm 3.4\%$
$T_w$	0.1°C	$\dot{Q}_w$	$\pm 4.5\%$	$\pm 1.4\%$
$T_a$	0.1°C	$\dot{Q}_a$	$\pm 5.6\%$	$\pm 3.1\%$
$T$	0.1°C	$j$	$\pm 12.1\%$	$\pm 6.1\%$

$$\frac{1}{U_{o,w}} = \frac{b'_r A_o}{h_i A_{p,i}} + \frac{b'_p x_p A_o}{k_p A_{p,m}} + \frac{1}{h_{o,w} \left( \frac{A_{p,o}}{b'_{w,p} A_o} + \frac{A_f \eta_{f,wet}}{b'_{w,m} A_o} \right)} \quad (1)$$

where

$$h_{o,w} = \frac{1}{\frac{C_{p,a}}{b'_{w,m} h_{c,o}}} \quad (2)$$

The tube-side heat transfer coefficient,  $h_i$ , is evaluated from the Gnielinski correlation [16]. The four quantities ( $b'_{w,m}$ ,  $b'_{w,p}$ ,  $b'_p$ , and  $b'_r$ ) in Eq. (1) involving enthalpy–temperature ratios must be evaluated in advance. Detailed evaluation of these four terms can be found from Wang et al. [1]. The heat transfer performance is in terms of the Colburn  $j$  factor, i.e.,

$$j = \frac{h_{c,o}}{G_c C_{p,a}} Pr^{2/3} \quad (3)$$

The determination of the mass transfer coefficient can be obtained from the process line [10]. Namely,

$$\frac{di}{dW} = Le \frac{i - i_w}{W - W_{S,w}} + (i_{g,t} - 2500.9 \times Le) \quad (4)$$

where the parameter,  $Le$ , is given as

$$Le = \frac{h_{c,o}}{h_d C_{p,a}} \quad (5)$$

Detailed integration of Eq. (4) can be found from Myers [15]. The reduction of the friction factor of the heat exchanger is evaluated from the pressure drop equation proposed by Kays and London [17] as

$$f = \frac{A_c \rho_i}{A_o \rho_m} \left[ \frac{2 \rho_i \Delta P}{G_c^2} - (1 + \sigma^2) \left( \frac{\rho_i}{\rho_o} - 1 \right) \right] \quad (6)$$

#### 4. Results and discussion

Fig. 3 shows the air side performances for type (I) louver under completely wet conditions ( $RH_{in} = 90\%$ ). The air side performances shown in the figure are in terms of sensible  $j$  factors and friction factors  $f$ . As seen, the heat transfer performance is relatively insensitive to change of fin pitch and the number of tube row. The results are analogous to the heat transfer performance under completely dry conditions [2–5]. However, contrary to the test results of heat transfer performance, a significant effect of fin pitch on the friction performance is observed. The friction factors for

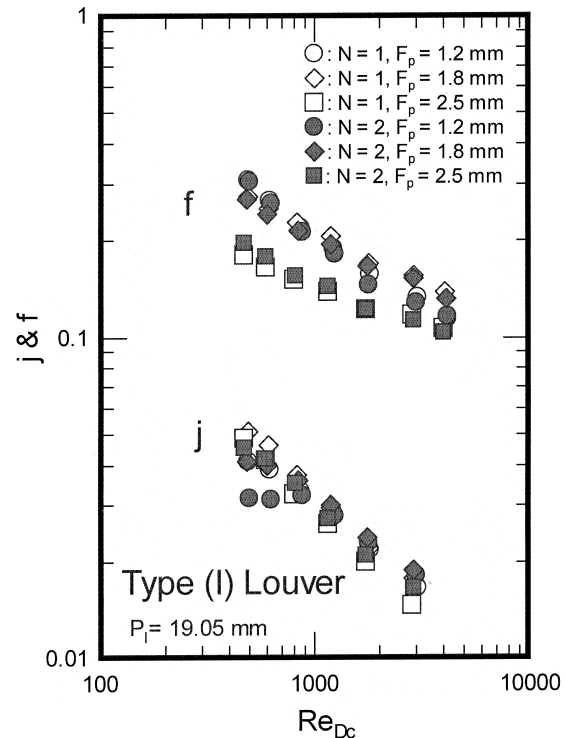


Fig. 3. Air side performances for type (I) louver.

$F_p = 1.2$  mm are about 30–50% higher than those of  $F_p = 2.5$  mm. For various louver fin patterns operated at fully dry conditions, Chang et al. [2] and Wang et al. [3–5] reported that the effect of fin pitch on the friction performance is again relatively small. There are several possible explanations of the difference among dry and wet conditions. Firstly, when fin-and-tube heat exchangers are operated at the dehumidifying conditions, water vapor condenses on fin surfaces. Consequently, the condensate retention may become severe as fin spacing is decreased. Secondly, as fin pitch is decreased, the condensate may considerably change the flow pattern across the heat exchanger. This phenomenon can be further explained by the flow visualization conducted by Yoshii et al. [18] under dehumidifying condition with a scale-up model of fin-and-tube heat exchanger, they noticed that the condensate adhere to both sides may cause the airflow within the channel to twist when the fin channel is close to each other. As a consequence, as shown in Fig. 4(a), the whirl flow is generated and may produce extra friction loss as fin spacing is decreased. Conversely, as shown in Fig. 4(b), the effect of twisted flow is comparatively small when the space between the fin channel is increased and the effect of fin pitch on the friction is decreased as  $Re_{D_c}$  is increased, as illustrated in Fig. 3. This is because of better mixing of airflow caused by the louver. Therefore, the effect of whirl flow is becoming relatively small.

Fig. 5 shows air side performance for type II louver under fully wet conditions. As seen, the air side performance for type II louver is similar to those of type (I) louver. The heat transfer performances for  $F_p = 2.5$  mm are lower than those of  $F_p = 1.2$  mm (except at the very low Reynolds region where the Coburn  $j$  factors are comparable for these different fin pitch). Note

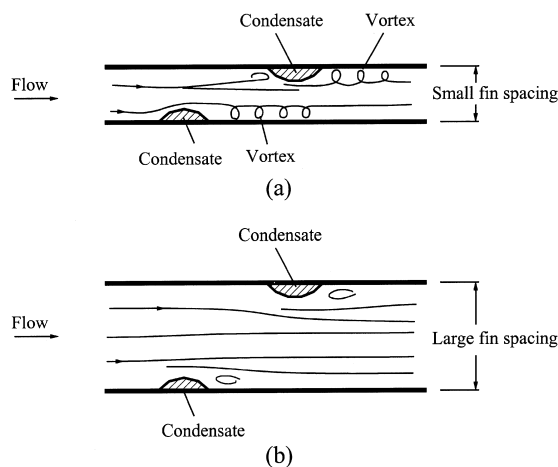


Fig. 4. Air flow pattern in presence of condensate.

that the louver number for type (II) is larger than those of type (I), the interaction between the louver and the blockage of the second row may provide better mixing condition of the airflow. As a result, comparing to the one-row configuration, the effect of fin pitch is less pronounced for  $N = 2$ .

Fig. 6 shows the effect of relative humidity ( $T_{db} = 27^\circ\text{C}$ ,  $\text{RH} = 50\%$  and  $90\%$ ) on the sensible  $j$  factors and friction factors for sample #1, #3, #9, and #10. As shown in the figure, the sensible heat transfer performances are relatively insensitive to change of inlet condition. The results are analogous to those reported earlier by Wang et al. [1]. Some investigators like Mirth and Ramadhyani [19,20] and Fu et al. [8] reported that the sensible heat transfer performance is related to the inlet conditions (relative humidity or dew point temperature). Wang et al. [1] pointed out the controversies are related to calculation of wet fin efficiency.

In addition to the sensible heat transfer performance, the effect of inlet relative humidity on friction factors for type (I) and type (II) louver is slightly different. As seen in Fig. 6, type (II) louver shows less dependence of inlet humidity than does type (I). Possible explanation may be related to their difference in longitudinal tube pitch  $P_1$ . Note that  $P_1 = 19.05$  mm for type (I) while  $P_1 = 22$  mm for type (II). For higher condensate loading ( $\text{RH}_{in} = 90\%$ ), larger longitudinal tube pitch will increase the effective spacing between

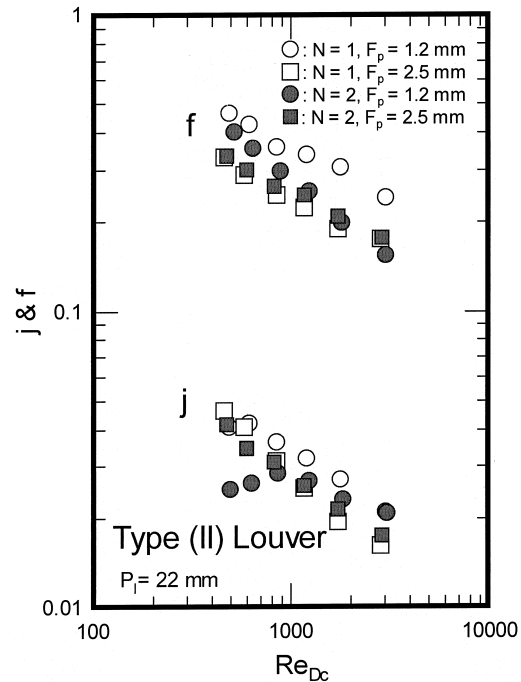


Fig. 5. Air side performances for type (II) louver.

tube row, and hence can be helpful to the condensate drainage problem. Wang et al. [1] also reported negligible effect of inlet condition on the friction performance and their longitudinal tube pitch is also 22 mm. For type (I) louver,  $P_1 = 19.05$  mm, the friction factors for  $RH_{in} = 90\%$  are approximately 5–25% higher pressure drops than those at  $RH_{in} = 50\%$ .

The dehumidifying process involves heat and mass transfer simultaneously, it is convenient to employ the analogy between heat and mass transfer if mass transfer data are unavailable because the conduction and diffusion in a liquid are governed by physical laws of identical mathematical form. Such an analogy is widely used in a form recommended by Chilton and Coburn in 1934, i.e.  $h_{c,o}/h_d C_p = (Sc/Pr)^{-2/3}$ , which is quite adequate for most external flow but is inappropriate for fully developed laminar duct flows [21]. For fin-and-tube heat exchangers, most of the open literatures showed that

$$\frac{h_{c,o}}{h_d C_p} \approx 1 \tag{7}$$

The experimental data of Hong [22] indicated that this value is between 0.7 and 1.1, Seshimo et al. [23] gave a value of 1.1. Eckels and Rabas [24] reported also the relevance in their plain fin-and-tube heat exchangers. Wang and Chang [9] found that the value of  $h_{c,o}/h_d C_p$  increases slowly with Reynolds number and developed

the following correlation:

$$\frac{h_{c,o}}{h_d C_p} = 0.57 Re_{D_h}^{0.07} \tag{8}$$

where

$$D_h = \frac{4A_c L}{A_o} \tag{9}$$

In the present study, Eq. (7) is roughly applicable. However, the values of  $h_{c,o}/h_d C_p$  for higher inlet relative humidity would be lower than that for lower inlet humidity. The results implies mass transfer coefficients will be higher for a higher inlet humidity. For gas absorption in a liquid falling film inside a vertical tube, Kafesjian et al. [25] found that the mass transfer performance is related to the gas Reynolds number, Schmidt number, and film Reynolds number,  $(4\Gamma/\mu_f)$ . i.e.

$$Sh_{D_h} = 0.00814 Re_{D_h}^{0.83} Sc^{0.44} \left( \frac{4\Gamma}{\mu_f} \right)^{0.15} \tag{10}$$

where  $\Gamma$  is the film flow rate per unit width. Eq. (10) gives higher values than those given by the analogy. The film Reynolds number may play a significant role in the mass transfer coefficients. For the present test condition, condensation of humid air along the heat exchanger inside the fin-and-tube heat exchange is

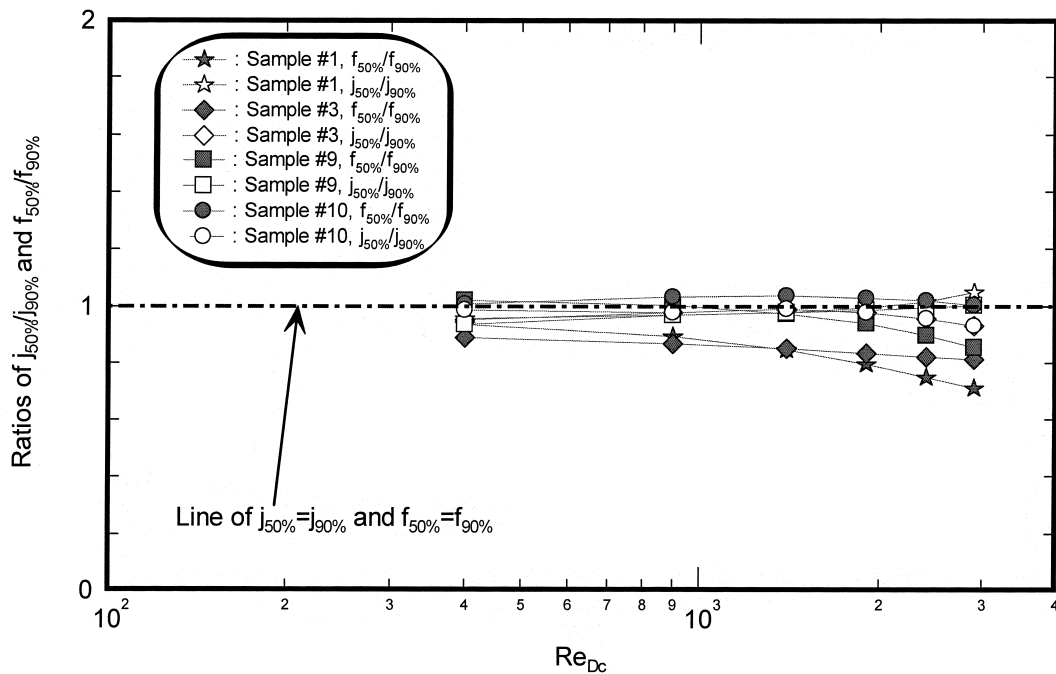


Fig. 6. Effect of inlet humidity on the heat transfer and friction performance.

much more similar to channel flow. In addition, film flow caused by the condensate may alter the applicability of Eq. (7). Consequently, it is necessary to modify Eq. (7) to increase the scope of applicability. Higher condensate loading is expected for a higher inlet humidity condition. The mean condensate film Reynolds number (evaluated based on the periphery of tube) ranges from 0.5 to 10 ( $2\Gamma/\mu_f$ ) in the present study. As a result, the film Reynolds number and the associated geometrical parameters were taken into account which result in a modification to the analogy. i.e.,

$$\frac{h_{c,o}}{h_d C_p} = 0.2702 Re_{D_c}^{0.1739} \left( 0.6 + 0.8493 \left( \frac{2\Gamma}{\mu_f} \right)^{-0.1652 \exp(F_p/D_c)} \left( \frac{F_p}{P_1} \right)^{0.1984} N^{-0.501} \right) \quad (11)$$

Eq. (11) is applicable to both type (I) and type (II) louver, and is valid for  $RH_{in} = 50\text{--}90\%$ . Eq. (11) gives a mean deviation of 7.91% of the present database.

It is obvious from the curves shown in Figs. 3 and 5 that no single curve can be expected to describe the complex behaviors for both  $j$  and  $f$  factors. In addition, as seen in Fig. 4, a different behavior in friction is seen between type (I) and type (II). As a result, a multiple linear regression technique in a practical range of experimental data ( $400 < Re_{D_c} < 3000$ ) was carried out. The major characteristics length used for developing correlation is tube collar diameter. The use of either tube collar diameter or hydraulic diameter as the characteristics length is arbitrary as discussed by Webb [26]. However, use of tube diameter is much more appropriate to correlate the experimental data, and most of the successful correlations were based on fixed dimensions like tube diameter since it is more practical in application. The final correlations for  $j$  and  $f$  are given there by as follows:

$$j = 9.717 Re_{D_c}^{j1} \left( \frac{F_p}{D_c} \right)^{j2} \left( \frac{P_1}{P_t} \right)^{j3} \log_e \left( 3 - \frac{L_p}{F_p} \right)^{0.07162} N^{-0.543} \quad (12)$$

where

$$j1 = -0.023634 - 1.2475 \left( \frac{F_p}{D_c} \right)^{0.65} \left( \frac{P_1}{P_t} \right)^{0.2} N^{-0.18} \quad (13)$$

$$j2 = 0.856 \exp(\tan \theta) \quad (14)$$

$$j3 = 0.25 \log_e(Re_{D_c}) \quad (15)$$

and

$$f = 2.814 Re_{D_c}^{f1} \left( \frac{F_p}{D_c} \right)^{f2} \left( \frac{P_1}{P_t} \right)^{f3} \left( \frac{P_1}{P_t} + 0.091 \right)^{f4} \left( \frac{L_p}{F_p} \right)^{1.958} N^{0.04674} \quad (16)$$

where

$$f1 = 1.223 - 2.857 \left( \frac{F_p}{D_c} \right)^{0.71} \left( \frac{P_1}{P_t} \right)^{-0.05} \quad (17)$$

$$f2 = 0.8079 \log_e(Re_{D_c}) \quad (18)$$

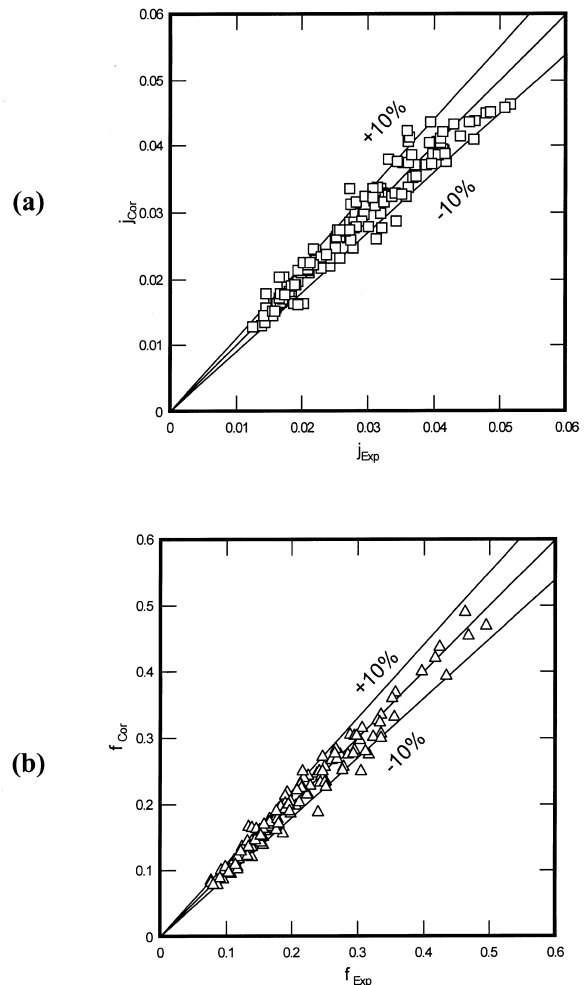


Fig. 7. Comparison of the proposed correlations with experimental data (a)  $j$  and (b)  $f$ .

$$f3 = 0.8932 \log_e(Re_{D_c}) \quad (19)$$

$$f4 = -0.999 \log_e\left(\frac{2\Gamma}{\mu_f}\right) \quad (20)$$

Rang of applicability for Eqs. (12) and (16) are as follows:

$Re_{D_c}$	400–3000
$P_t$	25.4 mm
$P_l$	19–22 mm
$D_o$ (before expansion)	9.53 mm
Fin pitch	1.2–2.5 mm
Louver angle	24.4–28.2 deg

As shown in Fig. 7, the proposed heat transfer and friction correlation (Eqs. (12) and (16)), can describes 80.5% and 85.3% of the experimental  $j$  and  $f$  within  $\pm 10\%$ , and the Eq. (12) gives a mean deviation of 5.94% while 6.1% for Eq. (16). Detailed comparisons between the proposed correlations of  $j$ ,  $f$  and  $h_{c,o}/h_d C_p$  and the experimental data are depicted in Table 3.

## 5. Conclusion

The air side performances of louvered fin surface under dehumidifying conditions were presented and discussed in this study. A total of 10 fin-and-tube heat exchangers having louver fin patterns were tested and compared. The following conclusions are made:

- The friction factors for louver fin increase with decrease of fin pitch.
- The effect of inlet condition on the friction performance is different between type (I) and type (II) louver. Type (II) louver shows less dependence of inlet condition (relative humidity) than does type (I) louver for its larger longitudinal tube pitch.
- The sensible heat transfer performance is insensitive to change of inlet relative humidity.
- The condensate film Reynolds number plays a significant role in the mass transfer and characteristics.

Table 3  
Comparison of the proposed correlation with the experimental data<sup>a,b</sup>

Deviation	$\pm 10\%$	$\pm 15\%$	$\pm 20\%$	$\pm 25\%$	Mean deviation
$j$	84.2%	93.2%	98.7%	99.1%	5.94%
$f$	81.2%	94.7%	97.0%	98.3%	6.1%
$h_{c,o}/h_d C_p$	68.7%	87.0%	93.9%	98.3%	7.89%

<sup>a</sup> Mean deviation =  $\frac{1}{M}(\sum_1^M \frac{|\text{Correlation}-\text{Data}|}{\text{Data}}) \times 100\%$ .

<sup>b</sup>  $M$ : number of data point.

For type (I) louver having smaller  $P_l$ , the friction performance is also related to the condensate film Reynolds number.

- A correlation of heat, momentum, and mass transfer was proposed which can correlate the present data-base with a mean deviation of 5.94%, 6.1%, and 7.89%, respectively.

## Acknowledgements

The authors would like to express gratitude for the financial support from the Energy R & D Foundation funding from the Energy Commission of the Ministry of Economic Affairs, Taiwan.

## References

- [1] C.C. Wang, Y.C. Hsieh, Y.T. Lin, Performance of plate finned tube heat exchangers under dehumidifying conditions, ASME J. of Heat Transfer 119 (1997) 109–117.
- [2] W.R. Chang, C.C. Wang, W.C. Tsi, R.J. Shyu, Air side performance of louver fin heat exchanger, in: Proceedings of the Fourth ASME/JSME Thermal Engineering Joint Conference, vol. 4, 1995, pp. 372–467.
- [3] C.C. Wang, Y.P. Chang, K.U. Chi, Y.J. Chang, An experimental study of heat transfer and friction characteristics of typical louver fin-and-tube heat exchangers, Int. J. of Heat and Mass Transfer 41 (1998) 817–822.
- [4] C.C. Wang, Y.P. Chang, K.U. Chi, Y.J. Chang, A study of non-redirection louver fin-and-tube heat exchangers, Proceeding of Institute of Mechanical Engineering, Part C., Journal of Mechanical Engineering Science 212 (1998) 1–14.
- [5] C.C. Wang, C.J. Lee, C.T. Chang, Y.J. Chang, Some aspects of the fin-and-tube heat exchangers: with and without louvers, J. of Enhanced Heat Transfer (1999), in press.
- [6] C.C. Wang, C.J. Lee, C.T. Chang, S.P. Lin, Heat transfer and friction correlation for compact louvered fin-and-tube heat exchanger, Int. J. of Heat and Mass Transfer 42 (1999) 1945–1956.
- [7] T. Senshu, T. Hatada, K. Ishibane, Heat and mass transfer performance of air coolers under wet conditions, ASHRAE Transactions 87 (2) (1981) 109–115.
- [8] W.L. Fu, C.C. Wang, C.T. Chang, Effect of anti-corrosion coating on the thermal characteristics of a louvered finned heat exchanger under dehumidifying condition, Advances in Enhanced Heat/Mass Transfer and Energy Efficiency (1995) 75–81 (ASME HTD-Vol. 320/PID-Vol. 1).
- [9] C.C. Wang, C.T. Chang, Heat and mass transfer for plate fin-and-tube heat exchangers: with and without hydrophilic coating, Int. J. of Heat and Mass Transfer 41 (1998) 3109–3120.
- [10] J.L. Threlkeld, Thermal Environmental Engineering, Prentice-Hall, New York, 1970.

- [11] S.G. Kandlikar, Thermal design theory for compact evaporators, in: R.K. Kraus, et al. (Eds.), *Compact Heat Exchangers*, Hemisphere, New York, 1990, pp. 245–286.
- [12] ASHRAE Standard 41.2-1987, Standard methods for laboratory air-flow measurement, American Society of Heating, Refrigerating and Air-Conditioning Engineers, Atlanta, 1987.
- [13] ASHRAE Standard 41.1-1986, Standard method for temperature measurement, American Society of Heating, Refrigerating and Air-Conditioning Engineers, Atlanta, 1986.
- [14] R.J. Moffat, Describing the uncertainties in experimental results, *Experimental Thermal and Fluid Science* 1 (1988) 3–17.
- [15] R.J. Myers, The effect of dehumidification on the air-side heat transfer coefficient for a finned-tube coil, M.S. Thesis, University of Minnesota, Minneapolis, 1967.
- [16] V. Gnielinski, Equation for heat and mass transfer in turbulent pipe and channel flow, *Int. Chem. Eng* 16 (1976) 359–368.
- [17] W.M. Kays, A.L. London, *Compact Heat Exchanger*, 3rd ed., McGraw-Hill, New York, 1984.
- [18] T. Yoshii, M. Yamamoto, M. Otaki, Effects of dropwise condensate on wet surface heat transfer of air cooling coils, in: *Proceedings of the 13th Int. Congress of Refrigeration*, 1973, pp. 285–292.
- [19] D.R. Mirth, S. Ramadhyani, Prediction of cooling-coils performance under condensing conditions, *Int. J. of Heat and Fluid Flow* 14 (1993) 391–400.
- [20] D.R. Mirth, S. Ramadhyani, Correlations for predicting the air-side Nusselt numbers and friction factors in chilled-water cooling coils, *Experimental Heat Transfer* 7 (1994) 143–162.
- [21] A.F. Mills, *Heat and Mass Transfer*, Irwin, Homewood, IL, 1995, p. 844.
- [22] K. Hong, Fundamental characteristics of dehumidifying heat exchangers with and without wetting coating, Ph.D. Thesis, Department of Mechanical Engineering, The Pennsylvania State University, 1996.
- [23] Y. Seshimo, K. Ogawa, K. Marumoto, M. Fujii, Heat and mass transfer performances on plate fin and tube heat exchangers with dehumidification, *Transactions JSME* 54 (499) (1998) 716–721.
- [24] P.W. Eckels, T.J. Rabas, Dehumidification: on the correlation of wet and dry transport process in plate finned-tube heat exchangers, *ASME Journal of Heat Transfer* 109 (1987) 575–582.
- [25] P. Kafesjian, C.A. Plank, E.R. Gerhard, Liquid flow and gas phase mass transfer in wetted wall towers, *AIChE J* 7 (1961) 463–466.
- [26] R.L. Webb, *Principles of Enhanced Heat Transfer*, Wiley, New York, 1994, pp. 131–133.